ESTIMATES OF THE LUNAR SURFACE COMPOSITION WITH CLEMENTINE IMAGES AND LSCC DATA. Yu. Shkuratov[1], C. Pieters[2], V. Omelchenko[1], D. Stankevich[1], V. Kaydash[1], L. Taylor[3], [1]Kharkov Astronomical Observatory, 35 Sumskaya St., Kharkov, 61022, Ukraine, Yuriy_Shkuratov@hotmail.com, [2]Geological Sciences, Brown University, Providence, Rhode Island, USA, [3]Planetary Geoscience Institute, University of Tennessee, Knoxville, Tennessee, USA.

Introduction: There have been several approaches to develop remote sensing technique to estimate composition of the lunar surface using multispectral observations. We present a new approach based on statistical analysis of spectral and compositional data for lunar samples by the Lunar Soil Characterization Consortium (LSCC) and using the UVVIS Clementine data with 1 km resolution. This technique allows us to estimate and map the abundance of TiO_2, SiO_2, and FeO, pyroxene and plagioclase content, and maturity degree (I_s/FeO).

Data and Their Analysis: We use data for LSCC -characterized mare soils of the Apollo-11, 12, 15, and 17 missions [1] and recent data for several Apollo-14 and -16 soils (highland regolith). Coordinated compositional and spectral measurements were carried out for samples with controlled particle size: <10 μm, 10-20 μm, and 20-45 μm. We used 42 samples for analysis. Bi-directional spectra were obtained with the RELAB spectrometer in the spectral range 300–2600 nm [2]. We have transposed the soil spectra to the Clementine spectral bands (415, 750, 900, 950, and 1000 nm).

The main point of our approach is to find relationships that provide the highest correlation coefficients between different linear combinations of optical parameters, on one hand, and chemical/mineral composition and degree of maturity, on the other hand. We used the following optical parameters: albedo $A_R = A(750\text{ nm})$, color-indexes: $C_{BR} = A(415\text{ nm}) / A(750\text{ nm})$, $C_{IR1} = A(900\text{ nm}) / A(750\text{ nm})$, $C_{IR2} = A(950\text{ nm}) / A(750\text{ nm})$, $C_{IR3} = A(1000\text{ nm}) / A(750\text{ nm})$, and bend $D = A(750\text{ nm})\,A(1000\text{ nm}) / [A(900\text{ nm})]^2$. An optimal empirical expression to derive high correlation coefficients is: $\log P = aA_R(\%)+bC_{BR}+cC_{IR1}+hC_{IR2}+eC_{IR3}+fD+g$, where P is a studied parameter. The weight coefficients a, b, c, h, e, f, and g minimize the RMS deviations of the calculated values of P from the measured values. Using the current set of LSCC data these coefficients are given in the following Table:

	a	*b*	*c*	*h*	*e*	*f*	*g*
TiO_2	-0.040	1.873	50.662	-17.747	-13.531	13.011	-32.542
FeO	-0.023	0.349	24.664	-15.632	-1.233	5.190	-11.968
SiO_2	0.002	-0.214	-2.091	-0.554	1.597	-0.736	3.511
Py	-0.023	0.079	16.771	-19.487	4.959	1.666	-2.782
Pl	0.016	0.861	-6.888	7.360	-1.527	-0.322	1.972
I_s/FeO	-0.013	-2.466	-35.496	17.736	5.303	-10.710	26.712

Our initial test of this approach used only 24 mare LSCC samples for calibration [3], it compares well with the present results. Comparison of the TiO_2 and FeO abundance maps with distributions obtained by *Lucey's et al.*technique [4] shows good correlation [5].

Results and Discussion: Determinations of lunar surface composition using the approach are illustrated here as maps.

Map of TiO_2. The predicted distribution of TiO_2 is presented in Fig. 1 (hereafter, dark color corresponds to low values of the mapped parameter). The range of TiO_2 variations, near 0.3–12%, seems to be quite reasonable. The highest abundance of TiO_2 can be found in Mare Tranquillitatis and Western Maria.

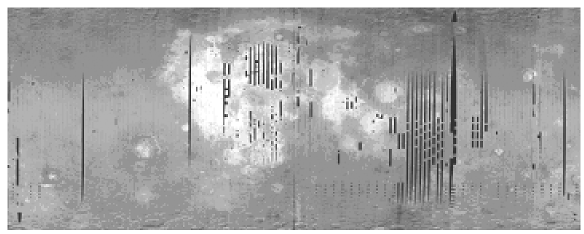

Fig. 1. Map of TiO_2.

Map of SiO_2. Variations of the parameter SiO_2 from 37% to 48% are shown in Fig. 2. The most ultrabasic material can be found in Western Maria. The lunar highlands are comparatively homogeneous for this parameter. In some cases the boundary between highlands and maria vanishes.

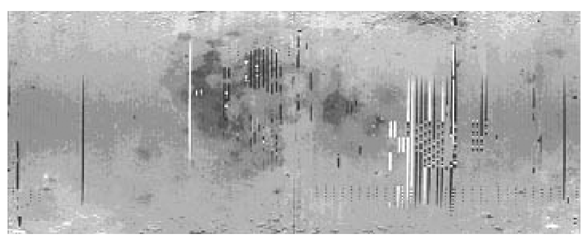

Fig. 2. Map of SiO_2.

From the equatorial band of relatively low SiO_2 and high TiO_2 these predictive parameters appear to somewhat sensitive to residual photometric errors in the UVVIS data.

Map of FeO. Our prediction for FeO distribution is shown in Fig. 3. As would be anticipated, highlands have significantly lower FeO abundance than maria. In many cases the FeO and TiO_2 boundaries are the same, reflecting correlation between these two parameters.

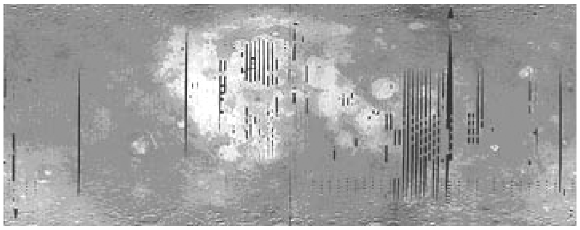
Fig. 3. Map of FeO.

Map of pyroxene. Fig. 4 shows a predicted distribution of pyroxene abundance. Our pyroxene map with the initial 1 km resolution shows that fresh lunar craters have higher abundance of pyroxenes than their surrounding soils. The South Pole – Aitken basin reveals higher general abundance of pyroxene than surroundings. We note also a strong correlation between the pyroxene and FeO distributions.

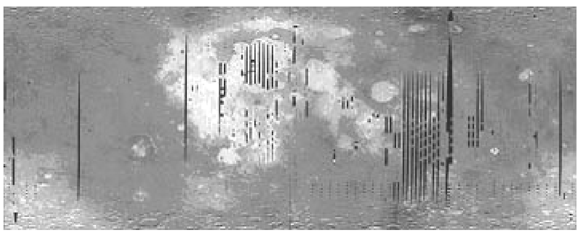
Fig. 4. Map of pyroxene.

Map of plagioclase. Distribution of plagioclase is presented in Fig. 5. As can be seen there is a strong correlation of this parameter with albedo, as it should be, since this parameter is sensitive to *crystalline* plagioclase. Fresh highland craters exhibit higher abundance of plagioclase than surrounding soils.

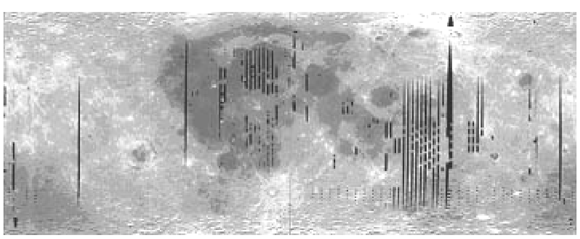
Fig. 5. Map of plagioclase.

Map of maturity degree. Fig. 6 shows a distribution of values for the maturity parameter, I_s/FeO. Young craters (their ejecta and rims) have low maturity degree. For mare regions, the map of I_s/FeO exhibits a similarity to the pyroxene map when comparing craters to background. This is natural, as the amount of crystalline material should correlate with regolith maturity. We note that the difference between mare and highland regions for the parameter I_s/FeO is rather small.

Using the map of I_s/FeO with the initial 1 km resolution we notice appreciable variations of the predicted maturity degree in mare regions. This can partially be due to a correlation of the parameters I_s/FeO and particle size. Actually, nano-phase iron grains, amount of which is characterized by the ratio I_s/FeO, are formed by a few processes such as in-melt reduction with hydrogen, selective sputtering, and selective condensation of vaporization products resulting from micro-impacts [6]. If the value I_s is related to surface condensation processes as expected [1], it would correlate with the total area of the surface particles. FeO bulk abundance is a function of the total volume of particles. Thus, the ratio I_s/FeO should be a function of particle size [6].

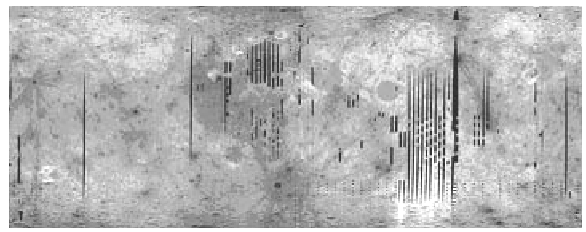
Fig. 6. I_s/FeO.

Conclusion: We represent a new empirical approach for remote sensing determination of lunar surface composition that gives reasonable and useful results. Nevertheless, further tests of accuracy limits need to be made. As with previous empirically-based techniques, we recognize the validity of results are restricted by inherent limits of compositional links to partial spectral data as well as the scope of sample data available to constrain parameters. A good example of accuracy limits of multispectral data is the difficulty of fully predicting the composition of the very low-Ti basalt of Luna-24 in Mare Crisium. Refinement and testing of the approach described here will proceed as additional LSCC data become available (Apollo and Luna). We intend to apply the technique to multispectral images of the Moon from the incoming ESA mission, SMART-1.

Acknowledgments: This work was partially supported by INTAS grant # 2000-0792. Research support from NASA grant NAG5-10469 (CMP) is gratefully acknowledged.

References: [1] Taylor L. et al. (2001). *JGR 106 (E11)*. 27,985-28,000, [2] Pieters C. et al. (2002). *Icarus. 155*. 285-298. [3] Shkuratov Yu. et al. (2002). *Abstr. pap. 36-th Inter. Microsymp. on Planetology, 14-16 October. 2002*, Moscow, abstract # MS090. [4] Lucey P. et al. (2000) *JGR 105 (E8)*. 20,297-20,306. [5] Omelchenko V. et al. *Abstr. pap. 36-th Inter. Microsymp. on Planetology, 14-16 October. 2002*, Moscow, abstract # MS074. [6] Morris R. (1977) *Proc. Lunar Sci. Conf. 8th*. 3719-3747.